

# Selective dissolution of magnetic iron oxides in the acid–ammonium oxalate/ferrous iron extraction method—I. Synthetic samples

Ingeborg H. M. van Oorschot and Mark J. Dekkers

*Utrecht University, Palaeomagnetic Laboratory 'Fort Hoofddijk', Budapestlaan 17, 3584 CD Utrecht, the Netherlands. E-mail: oorschot@geo.uu.nl*

Accepted 2001 January 15. Received 2001 January 12; in original form 2000 September 28

## SUMMARY

In soil magnetism, the magnetic parameters alone are not always sufficient to distinguish the lithogenic from the pedogenic magnetic fractions. Sequential extraction techniques have therefore been incorporated into magnetic studies to constrain the environmental interpretation. Here we report on the dissolution behaviour of magnetite and maghemite in the acid–ammonium oxalate method to see whether the method is suitable for specific dissolution of magnetic minerals from soils and sediments. To prevent changes in the extraction mechanism during the experiments (see Appendix A), we used an adapted version of the acid–ammonium oxalate (AAO) method, in which  $\text{Fe}^{2+}$  is added to the extraction solution prior to the experiment [the AAO-Fe(II) method]. The procedure was divided into several 30 min extraction steps to check the dissolution progress. Synthetic samples containing a quartz matrix with 0.1 wt per cent of iron oxides were extracted with the AAO-Fe(II) method. The iron oxides consisted of either magnetite or maghemite with grain sizes of  $<0.5 \mu\text{m}$  (fine grained or SD/PSD) and  $<5 \mu\text{m}$  (coarse grained or MD/PSD), or a 1:1 mixture of both minerals. Because only magnetite and maghemite were studied, the changes in magnetic characteristics could be monitored after each extraction step by analysis of the bulk susceptibility and hysteresis parameters measured at room temperature. The AAO-Fe(II) method preferentially dissolved the smaller iron oxides from the samples. For samples containing iron oxides with coarse grain size there is a preference for dissolving maghemite rather than magnetite. Extractions of the samples containing mixtures of two different grain sizes or with different mineralogy show that the method preferentially dissolves the smaller grains before attacking the coarse grains in the sample.

**Key words:** chemical extraction, environmental magnetism, maghemite, magnetic susceptibility, magnetite, rock magnetism.

## 1 INTRODUCTION

In environmental magnetism, palaeoclimate studies use the magnetic characteristics of sediments and soils to identify the climatic conditions that prevailed during their deposition or formation. It is possible to use magnetic climate proxies because first, iron is an important component in all rocks and their weathering products, and second, iron (hydr)oxide formation is strongly dependent on climatic factors such as rainfall and temperature (Maher 1998). Unfortunately, the magnetic signal alone is not always adequate for palaeoclimate reconstruction, and additional methods are needed to improve the interpretation of the magnetic parameters as climate proxy. Ideally, this is a method that can differentiate between maghemite and magnetite within soils.

These two iron oxides have a high magnetic signal compared to other magnetic iron oxides (for example, magnetite

has a saturation magnetization of  $92 \text{ Am}^2 \text{ kg}^{-1}$ , while that of haematite is  $0.4 \text{ Am}^2 \text{ kg}^{-1}$ ). This causes the magnetite and maghemite in natural samples often to control the overall magnetic signal. However, the differences in coercivity between maghemite and magnetite are very small and therefore these minerals can be difficult to distinguish by magnetic hysteresis methods only. Susceptibility and magnetization changes with temperature are difficult to interpret because natural maghemite can be thermally unstable due to differences in crystalline structure (for example, the substitution of iron by aluminium or titanium can decrease the Curie temperature of maghemite). Furthermore, organic carbon present in most natural soils will oxidize upon heating and thus can influence the signal.

In environmental magnetism as well as in soil science, it is imperative to differentiate between oxides formed as products of (recent) weathering and those inherited from the parent material. Within soil science, several sequential extraction techniques

have been developed that can identify iron (hydr)oxide phases such as total free iron (i.e. easily soluble iron) and X-ray amorphous iron. A technique that is frequently applied in environmental magnetism is the citrate–bicarbonate–dithionite (CBD) extraction method, which is reported to dissolve predominantly (fine-grained) maghemite (Verosub *et al.* 1993; Hunt *et al.* 1995; Sun *et al.* 1995). However, we have recently shown that the CBD method is only useful for identification of grain sizes of magnetite and maghemite in samples (van Oorschot & Dekkers 1999).

Therefore, we started an investigation to find other extraction methods that would selectively dissolve iron oxides. Here, we discuss results of extractions of well-defined synthetic samples with the acid–ammonium oxalate/ferrous iron [AAO-Fe(II)] extraction method (results of extractions of natural samples will be discussed in a future paper). The AAO method is reported to extract only the X-ray amorphous iron oxides from soils (Schwertmann 1964; McKeague & Day 1965; Fischer 1972; Cornell & Schindler 1987; Phillips & Lovley 1987) and therefore has potential for application in environmental magnetism where it could be used to dissolve the secondary iron oxides from soils.

The original AAO extraction technique uses a mixture of oxalic acid and ammonium oxalate, and was introduced by Tamm (1922, 1932). Schofield (1949) and Deb (1950) showed that the method, when performed in daylight, dissolved the same phases as dithionite (free iron oxides), but to a lesser extent. In UV light, the dissolution of free iron oxides by the AAO method was more extensive, and was shown to be caused by photocatalytic dissolution of iron oxides with oxalate (De Endredy 1963). Schwertmann suggested excluding light from the extraction experiments and demonstrated that only the X-ray amorphous iron oxides are dissolved when the method is performed in the dark (Schwertmann 1959, 1964). Other studies confirmed his results (McKeague & Day 1965; McKeague *et al.* 1971).

The AAO method—as described by Schwertmann (1964)—has been frequently applied in soil science as well as in some environmental magnetism studies to determine the amorphous and poorly crystalline iron oxide content of soils (e.g. Torrent *et al.* 1980; Olson & Ellis 1982; Schwertmann *et al.* 1982, 1985; Phillips & Lovley 1987; Fine & Singer 1989; Borggaard 1990; Canfield *et al.* 1992; Golden *et al.* 1994; Pinheiro-Dick & Schwertmann 1996; Rozan *et al.* 1997). However, several studies have shown that crystalline iron oxides can be dissolved as well with the AAO method (e.g. McKeague *et al.* 1971; Schwertmann 1973; Walker 1983; Borggaard 1988, 1990; Fine & Singer 1989). Others reported that the method can be applied to dissolve specific minerals, such as magnetite, and that differentiation on the basis of mineralogy would be possible with this method (Chao & Zhou 1983; Golden *et al.* 1994). These results contrast with the original observation that the AAO method only dissolves amorphous iron oxides. In the method proposed by Schwertmann (1964) the dissolution rate changes with time. This change in dissolution rate is related to the increasing concentration of  $\text{Fe}^{2+}$  in the extraction solution during the extraction time (Fischer 1972; see also Appendix A). A constant dissolution rate can be established by the addition of a small amount of  $\text{Fe}^{2+}$  to the extraction solution prior to the experiment (e.g. Fischer 1972; Blesa *et al.* 1987; Sulzberger *et al.* 1989; Grygar 1997). This adapted method was used in our experiments and will be referred to as the AAO-Fe(II) method.

Further aspects of this change in dissolution rate as well as the different extraction mechanisms of the AAO method are summarized in Appendix A.

We tested whether the AAO-Fe(II) method would dissolve crystalline iron oxides from synthetic samples by extracting dispersions of well-defined crystalline iron oxides in a quartz matrix. Furthermore, we studied whether the method would selectively dissolve specific minerals from our samples by conducting extractions of mixtures of iron oxides of different mineralogies.

## 2 MATERIALS AND METHODS

### 2.1 Extraction method

The procedure we use is based on the method of Schwertmann (1964) and the modifications described by Grygar (1997). It involves the use of a 20 mM acid–ammonium oxalate solution with 2 mM  $\text{Fe}^{2+}$  added, as described in the extraction scheme of Fig. 1. Table 1 compares the parameters of our procedure to those of Schwertmann and Grygar.

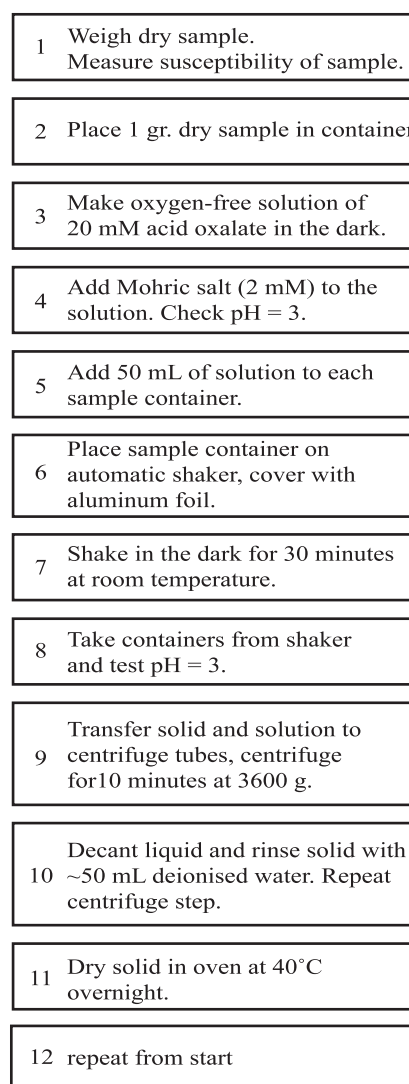


Figure 1. Flowchart of the AAO-Fe(II) extraction method as used in the experiments of this study.

**Table 1.** Specifications for three different methods of acid–ammonium oxalate extraction.

	Schwertmann (1964)	Grygar (1997)	This study
Purging gas	none	nitrogen	argon
pH	3	2.7	3
Concentration ferrous iron	none	2 mM	2 mM
Concentration acid ammonium oxalate	200 mM	20 mM	20 mM
Volume of solution	100 mL	–	50 mL
Extraction time	2 hr	–	30 min (per step)
Sample mass	1–5 g soil	5 mg iron oxide	1 g synthetic sample 1 wt% iron oxides

The extraction solution was prepared with deoxygenated water to prevent oxidation of  $\text{Fe}^{2+}$  in the extraction solution. The oxygen was removed from the water by boiling deionized water ( $\sim 1.5$ – $2$  L) until approximately 1 L was left; this was subsequently purged with Ar gas ( $\sim 1$  hr for 1 L of water) and simultaneously cooled down to room temperature. This water was used to make a 1 L solution of 0.02 M oxalic acid/ammonium oxalate at pH 3 by adding 1.6 g ammonium oxalate  $[(\text{NH}_4)_2\text{C}_2\text{O}_4 \cdot \text{H}_2\text{O}]$  and 1.1 g oxalic acid  $(\text{H}_2\text{C}_2\text{O}_4 \cdot 2\text{H}_2\text{O})$ . Since pH plays an important role in the extraction mechanism (see Appendix A), it was regularly checked throughout the preparation and extraction experiment. The bottle containing the solution was wrapped in aluminium foil to prevent photo-excitation of the oxalate, and the solution was continuously purged with Ar gas throughout the preparation. The  $\text{Fe}^{2+}$  was then added in the form of 0.784 g Mohr salt  $[\text{Fe}(\text{NH}_4)_2(\text{SO}_4)_2 \cdot 6\text{H}_2\text{O}]$  to make a concentration of 2 mM  $\text{Fe}^{2+}$  in solution. For each 1 g sample, 50 mL of this solution was required to perform one extraction step. A total of 12 samples as well as two blank samples were used for each sample series, requiring 700 mL of solution per extraction step. For each step a new solution was prepared.

After checking the pH of the solution, 50 mL was added with a dispenser to each of the sample containers. These 100 mL sample containers are made of brown glass, which prevents photo-catalytic dissolution of iron oxides during extraction. Subsequently, the containers were closed and placed on a mechanical shaker (Marius, type 71 SL) at room temperature at medium speed for 30 min. Aluminium foil was wrapped around the containers and the shaker to prevent photochemical dissolution. After 30 min the samples were transferred to centrifuge tubes, and the liquid and solid phases were separated by centrifuging for 10 min at 3600 g ( $\sim 4417$  rpm, the centrifuge was an MSE Mistral 2000). The liquid was decanted (after checking pH, which remained at 3 for all samples) and the samples were rinsed with  $\sim 50$  mL deionized water and centrifuged again. The remaining solid was dried in air in an oven at  $40^\circ\text{C}$  for  $\sim 12$  hr. The extraction step was repeated a maximum of twice, each sample series requiring one day for extraction and drying of the samples.

## 2.2 Synthetic samples

To keep control of as much of the experimental parameters as possible, we used synthetic samples made from a matrix of quartz (analytical grade, Merck) to which iron oxides were added. The

quartz grains had an average grain size of 0.2–0.8 mm and contained  $<0.05$  per cent substances soluble in hydrochloric acid. The starting mass of the samples was  $\sim 1$  g and the concentration of iron oxides was  $\sim 0.1$  wt per cent.

The iron oxides were taken from a study by Hartstra (1982a); in addition, we prepared fine-grained iron oxides according to the method described in Schwertmann & Cornell (1991). Table 2 shows the properties of these oxides. The data for the natural iron oxides compare well with the original analyses by Hartstra (1982a) (see Table 3). The iron oxides were mixed with the matrix material by stirring both components in acetone in an ultrasonic bath for approximately 2 min (van Oorschot & Dekkers 1999). After stirring, the samples were dried overnight in air in an oven at  $40^\circ\text{C}$  and stored. The samples contained either one of the mentioned iron oxides or a mixture of two of these oxides (see Table 4). Each sample series consisted of 12 samples and two blanks. The blanks contained only quartz and were handled in the same way as the other samples. After preparation the samples were transferred to the sample containers.

## 2.3 Magnetic methods

Prior to the start of the experiment and after each extraction step, the dry samples were weighed and bulk susceptibility as well as hysteresis parameters of the samples were measured. Bulk susceptibility was measured with a KLY-2 susceptibility bridge (AGICO). The sensitivity of the equipment is  $4 \times 10^{-8}$  SI, and

**Table 2.** Properties and origin of the iron oxides used in this study. Synthetic iron oxides were made according to Schwertmann & Cornell (1991), while the natural samples were taken from a study by Hartstra (1982a).

Synthetic iron oxides	Natural iron oxides
Magnetite – grain size $<0.5 \mu\text{m}$ – $T_c \sim 580^\circ\text{C}$	Maghemite – grain size $<0.5 \mu\text{m}$ – $T_c \sim 580^\circ\text{C}$
Magnetite – grain size $<5 \mu\text{m}$ – $T_c \sim 640^\circ\text{C}$	Titanomaghemite – grain size $<5 \mu\text{m}$ – $T_c \sim 550^\circ\text{C}$ – $\text{Fe}_{(2-x)}\text{Ti}_x\text{O}_3$ ( $x=0.05$ , $z=0.8$ )

**Table 3.** Initial susceptibility and hysteresis parameters of the iron oxides used in our study (column B). The data come from samples of iron oxides mixed with quartz (typically  $\sim 1$  mg iron oxides in a 1 g sample). Data for the  $<5 \mu\text{m}$  iron oxides are compared to data published by Hartstra (1982a, 1982b) in column A and data from Vlag *et al.* (1996) in column C.

Iron oxide	$\chi_0$ [ $10^{-8} \text{ m}^3 \text{ kg}^{-1}$ ]			$M_{rs}$ [ $\text{A m}^2 \text{ kg}^{-1}$ ]			$M_s$ [ $\text{A m}^2 \text{ kg}^{-1}$ ]			$B_{cr}$ [mT]			$B_c$ [mT]			$M_{rs}/M_s$			$B_{cr}/B_c$			
	A	B	C	A	B	C	A	B	C	A	B	C	A	B	C	A	B	C	A	B	C	
Syn. magnetite		82.4			0.028			0.160			25.7			12.3			0.20			2.4		
Syn. maghemite		54.4			0.029			0.106			27.3			15.4			0.29			1.8		
Nat. magnetite	53.6	58.0		0.011	0.018		0.065	0.121		39.7	32.1	40	14.3	12.8	15.0	0.17	0.15	0.18	2.8	2.5	2.7	
Nat. titanomaghemite	19.4	19.8		0.010	0.018		0.028	0.070		56.3	53.4		33.0	24.8		0.02	0.28		1.7	2.2		

our data were at least a factor of two higher. The susceptibility after each extraction step was normalized to the starting value of the susceptibility of the respective samples to enable comparison between different sample series. The hysteresis loops were measured with an alternating gradient magnetometer (Micromag) with a saturation field of 500 mT and a field increment of 5 mT. At 500 mT all samples had reached saturation magnetization. The sensitivity of the Micromag was  $1 \text{ nAm}^2$ , which was in the same range as the values for the  $M_{rs}$  of our blanks as well as for some of the mixtures after two extraction steps. All other samples had magnetizations of at least one order of magnitude higher than the sensitivity of the Micromag. The accuracy of each Micromag measurement was 2 per cent versus the calibration and the calibration was checked after every six measurements. All measurements were 70 per cent slope-corrected because of the high diamagnetic signal from the matrix. Backfield demagnetization was performed in the same magnetometer with a field increment of 1 mT to a maximum field of  $-100 \text{ mT}$  to determine the coercivity of remanence. A definition of all magnetic parameters used in this paper can be found in the glossary of Appendix B.

### 3 RESULTS

In Section 3.1 the magnetic properties of all sample series prior to extraction are presented. Subsequently, the results obtained from extractions of samples containing either one type of iron oxide (series 1–4 in Table 4, Section 3.2) or mixtures of iron oxides (series 5–8 in Table 4, Section 3.3).

#### 3.1 Magnetic properties before extraction

The mass susceptibility of the original samples is given in Table 3. The hysteresis parameters (Table 5) show that all samples plot in different areas of the Day plot (Fig. 2b). Typical values for the coarse-grained magnetite are 0.15 for  $M_{rs}/M_s$  and 2.5 for  $B_{cr}/B_c$ , while coarse-grained titanomaghemite has values of 0.28 and 2.2 for  $M_{rs}/M_s$  and  $B_{cr}/B_c$ , respectively. For fine-grained magnetite and fine-grained maghemite, our values are 0.20 and 0.29 for  $M_{rs}/M_s$  and 2.4 and 1.8 for  $B_{cr}/B_c$ , respectively, which is within the range published for magnetite by Dunlop & Özdemir (1997). The samples containing maghemite have a higher  $M_{rs}/M_s$  and a lower  $B_{cr}/B_c$  ratio than those containing magnetite. Samples of iron oxides with the same mineralogy show slightly higher  $M_{rs}/M_s$  and lower  $B_{cr}/B_c$  ratios for samples with fine grain size. Coercivity is high for unextracted samples, especially for the natural titanomaghemite ( $B_{cr}=53.4 \text{ mT}$ ), and decreases via coarse-grained magnetite and fine-grained maghemite to the lowest value for the fine-grained magnetite ( $B_{cr}=25.7 \text{ mT}$ ). The data for the coarse-grained minerals compare well to those published by Hartstra (1982a) and Vlag *et al.* (1996).

#### 3.2 Changes of magnetic properties with extraction

##### 3.2.1 Susceptibility

After one extraction step, only a small percentage of the initial susceptibility remains in the samples containing fine-grained

**Table 4.** Composition of synthetic samples used in this study. All samples had a matrix of quartz and a total iron oxide concentration of 0.1 wt per cent. Total sample mass was 1.0 g and each series consisted of 12 samples.

Sample series	Wt% synthetic magnetite ( $\phi < 5 \mu\text{m}$ )	Wt% synthetic maghemite ( $\phi < 5 \mu\text{m}$ )	Wt% natural magnetite ( $\phi < 5 \mu\text{m}$ )	Wt% natural titanomaghemite ( $\phi < 5 \mu\text{m}$ )
Syn. MN	0.1	–	–	–
Syn. MH	–	0.1	–	–
Nat. MN	–	–	0.1	–
Nat. TiMH	–	–	–	0.1
mix 1	0.05	–	0.05	–
mix 2	0.05	–	–	0.05
mix 3	–	0.05	0.05	–
mix 4	–	0.05	–	0.05
blanks	–	–	–	–

**Table 5** Hysteresis parameters of samples before and after extraction. The number in the header indicates the number of extraction steps performed. All parameters are averages of 12 samples; the fine-grained samples were only extracted once.

Iron oxide	$M_{rs}$ [ $A\ m^2\ kg^{-1}$ ]			$M_s$ [ $A\ m^2\ kg^{-1}$ ]			$B_{cr}$ [mT]			$B_c$ [mT]			$M_{rs}/M_s$			$B_{cr}/B_c$		
	0	1	2	0	1	2	0	1	2	0	1	2	0	1	2	0	1	2
Syn. magnetite	0.028	0.001	–	0.16	0.01	–	25.7	14.1	–	12.3	6.8	–	0.20	0.13	–	2.4	2.0	–
Syn. maghemite	0.029	0.002	–	0.11	0.01	–	27.3	15.0	–	15.4	6.1	–	0.29	0.13	–	1.8	2.5	–
Nat. magnetite	0.018	0.007	0.004	0.12	0.06	0.04	32.1	19.5	17.7	12.8	7.3	6.6	0.15	0.12	0.11	2.5	2.6	2.8
Nat. titanomaghemite	0.018	0.005	0.003	0.07	0.03	0.03	53.4	18.3	15.7	24.8	6.0	5.6	0.28	0.14	0.12	2.2	3.0	2.6
Blank	0.001	0.001	0.001	0.004	0.005	0.009	18.3	13.4	19.9	7.6	5.3	4.9	0.12	0.10	0.07	2.4	2.6	4.1

iron oxides (Fig. 2). Loss of susceptibility is slightly higher for the samples with fine-grained magnetite than for those containing fine-grained maghemite. The susceptibility of the samples containing the coarse-grained iron oxides decreases more slowly.

After two extraction steps almost all of the initial susceptibility in the samples with coarse-grained titanomaghemite has been removed, while  $\sim 40$  per cent still remains in the samples containing coarse-grained magnetite.

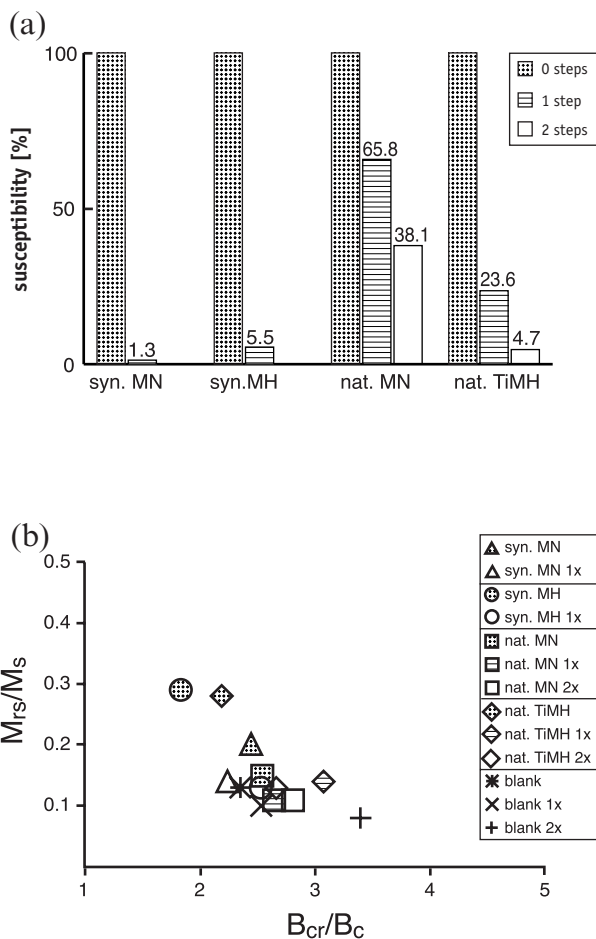


**Figure 2.** Magnetic parameters before and after extraction of synthetic samples containing a single type of iron oxide. Each sample series is represented by the average of 12 samples. The standard variation ranges between 0.9 and 4.8 per cent depending on extraction step and sample series. (a) Percentage of initial susceptibility remaining after each extraction step. (b) Day plot. MN indicates magnetite, MH indicates maghemite and TiMH indicates titanomaghemite. Fine-grained iron oxides prepared according to Schwertmann & Cornell (1991) are indicated with ‘syn’; coarse-grained iron oxides from the study of Hartstra (1982a) are indicated with ‘nat’.

### 3.2.2 Hysteresis parameters

The first extraction step causes the most significant change in hysteresis parameters (Table 5). The coercivities decrease to less than half the starting value for all fine-grained oxides and the coarse-grained titanomaghemite. The coercivity of the coarse-grained magnetite decreases to  $\sim 2/3$  of the original value. For the fine-grained samples,  $M_{rs}$  is reduced to less than 1 per cent of its original value after one extraction step. In the coarse-grained samples the reduction is  $\sim 50$  per cent for the magnetite and  $\sim 34$  per cent for the titanomaghemite.

A Day plot of the samples is given in Fig. 2(b). All samples shift from the pseudo-single-domain (PSD) to the multidomain (MD) range in the Day plot after extraction. This indicates that the PSD characteristics of the samples before extraction are most probably due to the contributions of a range of grain sizes, leading to an average grain size in the PSD range. During extraction the smallest grains are dissolved completely in the first extraction step, causing the average grain size to shift to a larger size. After two extraction steps, the samples with fine-grained iron oxides show resemblance in hysteresis parameters to the data of the blanks. The samples with coarse grains of natural titanomaghemite also compare well with the blanks. All extracted samples show a decrease in  $M_{rs}/M_s$  ratio. This decrease is strongest for the samples containing maghemite. All samples, except those containing fine-grained magnetite, show an increase in  $B_{cr}/B_c$  ratio after extraction. The decrease in  $M_{rs}/M_s$  ratio is related to a strong decrease of both  $M_{rs}$  and  $M_s$ , but the value of  $M_{rs}$  decreases more rapidly. The increase in  $B_{cr}/B_c$  is related to a more rapid decrease in  $B_c$ .

### 3.3 Dissolution behaviour of iron oxide mixtures

In Fig. 3(a), the decrease in susceptibility with each extraction step is given for all mixtures. The susceptibility of the mixtures after extraction mostly reflects the contribution of the coarse-grained samples, indicating that the fine-grained oxides were preferentially dissolved. The mixtures containing coarse-grained titanomaghemite show a more rapid decrease in susceptibility than those containing coarse-grained magnetite. The contribution of the fine-grained iron oxides to the susceptibility of

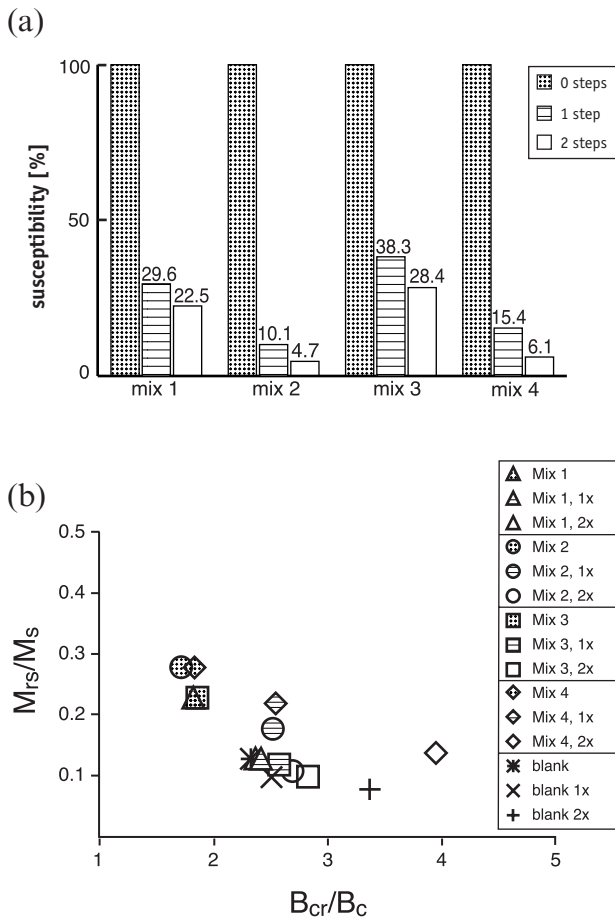


**Figure 3.** Magnetic parameters before and after extraction of synthetic samples containing a mixture of iron oxides. (a) Percentage of initial susceptibility remaining after each extraction step. (b) Day plot. Mix 1 and mix 3 are mixtures of coarse-grained magnetite with fine-grained magnetite and maghemite, respectively. Mix 2 and mix 4 are mixtures of coarse-grained titanomaghemite with fine-grained magnetite and maghemite, respectively. Fine-grained iron oxides prepared according to Schwertmann & Cornell (1991); coarse-grained iron oxides from the study of Hartstra (1982a). Each mixture is the average of a series of 12 samples. The standard deviation varies between 0.8 and 6.5 per cent depending on the extraction step and sample series.

the samples after extraction appears limited. However, judging from the percentage decrease in susceptibility for the different mixtures, the fine-grained maghemite dissolves more slowly from the samples than the fine-grained magnetite.

**Table 6.** Hysteresis parameters of samples after extraction. All parameters are averages of 12 samples. Mix 1 and mix 3 are mixtures of coarse-grained magnetite with fine-grained magnetite and maghemite, respectively. Mix 2 and mix 4 are mixtures of coarse-grained titanomaghemite with fine-grained magnetite and maghemite, respectively. The number in the header represents the number of extraction steps performed.

Sample	$M_{rs}$ [ $A\ m^2\ kg^{-1}$ ]			$M_s$ [ $A\ m^2\ kg^{-1}$ ]			$B_{cr}$ [mT]			$B_c$ [mT]			$M_{rs}/M_s$			$B_{cr}/B_c$		
	0	1	2	0	1	2	0	1	2	0	1	2	0	1	2	0	1	2
Mix 1 (syn. MN & nat. MN)	0.030	0.004	0.003	0.084	0.036	0.024	29.5	25.7	22.2	16.2	10.9	9.4	0.23	0.13	0.13	1.8	2.4	2.4
Mix 2 (syn. MN & nat. TiMH)	0.015	0.006	0.003	0.053	0.069	0.030	35.4	37.3	19.6	20.6	14.0	7.7	0.28	0.16	0.11	1.7	2.9	2.7
Mix 3 (syn. MH & nat. MN)	0.015	0.004	0.002	0.068	0.037	0.022	29.8	25.6	24.4	16.4	10.2	8.7	0.23	0.12	0.10	1.9	2.6	2.8
Mix 4 (syn. MH & nat. TiMH)	0.016	0.003	0.001	0.056	0.013	0.009	35.5	41.1	34.6	19.6	17.0	10.2	0.28	0.22	0.14	1.8	2.6	2.9
Blank	0.001	0.001	0.001	0.004	0.005	0.009	18.3	13.4	19.9	7.6	5.3	4.9	0.12	0.10	0.07	2.4	2.6	4.1

In Table 6 the hysteresis parameters of the mixtures before and after extraction are compiled. In all mixtures,  $M_{rs}$  is almost reduced to zero ( $\sim 10$  per cent of the starting value) after one extraction step, while  $M_s$  is reduced to approximately 50 per cent of its starting value. For those mixtures containing coarse-grained magnetite (mixtures 1 and 3),  $B_c$  and  $B_{cr}$  behave very similarly and decrease with each extraction step. For the samples with coarse-grained titanomaghemite (mixtures 2 and 4),  $B_{cr}$  increases after one extraction step, and has the lowest value after two extractions. This final decrease in  $B_{cr}$  is strongest for the mixture with fine-grained magnetite.  $B_c$  of these mixtures decreases with each extraction step, but the decrease is most rapid for the mixture containing fine-grained magnetite.

The hysteresis parameters of the mixtures are shown in Fig. 3(b). Before extraction, all mixtures plot in the same part of the diagram, in the PSD range close to the single-domain (SD) area. After extraction all samples show a decrease in  $M_{rs}/M_s$  ratio and an increase in  $B_{cr}/B_c$  ratio, and in the Day plot the samples move towards the MD area. This is an indication that the fine-grained oxides are preferentially removed from the mixture in the first extraction step, which changes the average grain size diameter to higher (more MD) values. The increase in coercivity ratio is strongest for the mixtures containing coarse-grained titanomaghemite, and weakest for the mixtures containing coarse-grained magnetite. The decrease in  $M_{rs}/M_s$  is strongest for the mixtures containing coarse-grained magnetite and weakest for the mixtures containing coarse-grained titanomaghemite. The fine-grained oxides do not appear to affect the hysteresis parameters of the extracted mixtures.

## 4 DISCUSSION AND CONCLUSIONS

### 4.1 Synthetic samples

We have shown that the AAO-Fe(II) method can dissolve crystalline iron oxides of varying grain sizes. However, the dissolution behaviour of each mineral type and grain size is very distinct and they can be identified by magnetic analysis of the samples before and after extraction. With one extraction step, almost all fine-grained iron oxides are removed from the samples.

The results of our experiments show that with a combination of susceptibility and hysteresis data we can distinguish grain size fractions as well as the mineralogy of coarse grains in samples before and after extraction. All single-oxide samples plot in different areas of the Day plot before extraction. After extraction we can make a distinction according to grain size from the

susceptibility data, where the susceptibility decreases most strongly for the fine-grained iron oxides. Furthermore, we can make a distinction between magnetite and titanomaghemite samples from the susceptibility data, which show that the coarse-grained magnetite has the slowest decrease in susceptibility after extraction. Based on the susceptibility decrease, the dissolution rate can be classified as follows: fine-grained iron oxides > coarse-grained titanomaghemite > coarse-grained magnetite.

The mineralogy and grain sizes of the mixtures can also be identified from the susceptibility data combined with the Day plot. The susceptibility data reflect the behaviour of the coarsest grain size fraction in the mixtures, and here we can again distinguish between magnetite and titanomaghemite. We also see a more rapid decrease in susceptibility (2–10 per cent more loss of starting susceptibility) for the mixtures containing fine-grained magnetite than for those with fine-grained maghemite. In the Day plot, the samples plot close together before extraction. However, the plot is useful to distinguish between the different mixtures after extraction. The data indicate that in mixtures of grain size and mineralogy the preferential dissolution pathway is fine-grained oxides first (with a slight preference for magnetite) and coarse-grained samples last (with a preference for titanomaghemite).

#### 4.2 Comparison with citrate–bicarbonate–dithionite extraction

Like the citrate–bicarbonate–dithionite (CBD) method, the AAO-Fe(II) method preferentially dissolves the fine-grained iron oxides from synthetic samples. However, the results of the AAO-Fe(II) method give more information about the type of iron oxides that are dissolved. The CBD method can only be used to differentiate fine from coarse grains (e.g. van Oorschot & Dekkers 1999), while the AAO-Fe(II) method can identify both grain size and mineralogy. The most important parameter in the CBD method is the extraction temperature (e.g. van Oorschot & Dekkers 1999); in the AAO-Fe(II) method light and pH can influence the extraction as well. The dissolution mechanism in the AAO-Fe(II) method is less aggressive and results give more detail than the CBD method; therefore, we would recommend this procedure for use in further studies.

#### 4.3 Implications for the future

The AAO-Fe(II) extraction method has good potential as a tool in environmental magnetism. It may be suitable to dissolve all fine-grained pedogenic iron oxides from palaeosol samples in one extraction step, while leaving the lithogenic iron oxides virtually untouched. Because of the slightly preferential dissolution of fine-grained magnetite over fine-grained maghemite, the method could possibly differentiate between magnetite and maghemite within the pedogenic and lithogenic fractions. Before it can be used in environmental magnetism, however, the method needs to be tested on natural samples.

#### ACKNOWLEDGMENTS

The manuscript was substantially improved by the constructive reviews of Dr Stanjek and Dr Kletetschka. This work was conducted under the programme of the Vening Meinesz Research School of Geodynamics (VMSG) and funded by the Netherlands Organization for Scientific Research (NWO/ALW).

#### REFERENCES

- Baumgartner, E., Blesa, M.A., Marinovich, H.A. & Maroto, A.J.G., 1983. Heterogeneous electron transfer as a pathway in the dissolution of magnetite in oxalic acid solutions, *Inorganic Chem.*, **22**, 2224–2226.
- Blesa, M.A., Marinovich, H.A., Baumgartner, E.C. & Maroto, A.J.G., 1987. Mechanism of dissolution of magnetite by oxalic acid-ferrous ion solutions, *Inorganic Chem.*, **26**, 3713–3717.
- Borggaard, O.K., 1981. Selective extraction of amorphous iron oxides by EDTA from soils from Denmark and Tanzania, *J. Soil Sci.*, **32**, 427–432.
- Borggaard, O.K., 1988. Phase identification by selective dissolution techniques, in *Iron in Soils and Clay Minerals*, pp. 83–98, eds Stucki, J.W., Goodman, B.A. & Schwertmann, U., Reidel, Dordrecht.
- Borggaard, O.K., 1990. Kinetics and mechanism of soil iron oxide dissolution in EDTA, oxalate and dithionite, *Sci. Géol. Mém.*, **85**, 139–148.
- Canfield, D.E., Raiswell, R. & Bottrell, S., 1992. The reactivity of sedimentary iron minerals toward sulfide, *Am. J. Sci.*, **292**, 659–683.
- Chao, T.T. & Zhou, L., 1983. Extraction techniques for selective dissolution of amorphous iron oxides from soils and sediments, *J. Soil Sci. Soc. Am.*, **47**, 225–232.
- Cornell, R.M. & Schindler, P.W., 1987. Photochemical dissolution of goethite in acid/oxalate solution, *Clays Clay Min.*, **35**, 347–352.
- Cornell, R.M. & Schwertmann, U., 1996. *The Iron Oxides*, VCH Publishers, Weinheim.
- De Endredy, A.S., 1963. Estimation of free iron oxides in soils and clays by a photolytic method, *Clay Min. Bull.*, **5**, 209–217.
- Deb, B.C., 1950. The estimation of free iron oxides in soils and clays and their removal, *J. Soil Sci.*, **1**, 212–220.
- Del Campillo, M.C. & Torrent, J., 1992. A rapid acid-oxalate extraction procedure for the determination of active Fe-oxide forms in calcareous soils, *Z. Pflanzenernahrung Bodenkunde*, **155**, 437–440.
- Dunlop, D.J. & Özdemir, Ö., 1997. *Rock Magnetism: Fundamentals and Frontiers*, Cambridge Studies in Magnetism, Cambridge University Press, Cambridge.
- Fine, P. & Singer, M.J., 1989. Contribution of ferrimagnetic minerals to oxalate- and dithionite-extractable iron, *J. Soil Sci. Soc. Am.*, **53**, 191–196.
- Fischer, W.R., 1972. Die Wirkung von zweiwertigem Eisen auf Lösung und Umwandlung von Eisen (III)-hydroxiden, in *Pseudogley and Gley—Genesis and Use of Hydromorphic Soils*, pp. 37–44, eds Schlichting, E. & Schwertman, U., VCH Publishers, Weinheim.
- Golden, D.C., Ming, D.W., Bowen, L.H., Morris, R.V. & Lauer, H.V., 1994. Acidified oxalate and dithionite solubility and color of synthetic, partially oxidized Al-magnetites and their thermal oxidation products, *Clays Clay Min.*, **42**, 53–62.
- Grygar, T., 1997. Dissolution of pure and substituted goethites controlled by the surface reaction under conditions of abrasive stripping voltammetry, *J. Solid State Electrochem.*, **1**, 77–82.
- Hartstra, R.L., 1982a. Grain-size dependence of initial susceptibility and saturation magnetization-related parameters of four natural magnetites in the PSD-MD range, *Geophys. J. R. astr. Soc.*, **71**, 477–495.
- Hartstra, R.L., 1982b. Some rockmagnetic parameters for natural iron-titanium oxides, *PhD thesis*, Utrecht University, Utrecht.
- Hering, J.G. & Stumm, W., 1990. Oxidative and reductive dissolution of minerals, in mineral–water interface geochemistry, in *Reviews in Mineralogy*, pp. 427–465, eds Hochella, M.F. & White, A.F., Mineralogical Society of America, Washington, DC.
- Hunt, C.P., Singer, M.J., Kletetschka, G., TenPas, J. & Verosub, K.L., 1995. Effect of citrate–bicarbonate–dithionite treatment on fine-grained magnetite and maghemite, *Earth planet. Sci. Lett.*, **130**, 87–94.
- Maher, B.A., 1998. Magnetic properties of modern soils and Quaternary loessic paleosols: paleoclimatic implications, *Palaeogeogr., Palaeoclimat., Palaeoecol.*, **137**, 25–54.

- McKeague, J.A. & Day, J.H., 1965. Dithionite- and oxalate-extractable Fe and Al as aids in differentiating various classes of soils, *Can. J. Soil Sci.*, **46**, 13–22.
- McKeague, J.A., Brydon, J.E. & Miles, N.M., 1971. Differentiation of forms of extractable iron and aluminum in soils, *Proc. Soil Sci. Soc. Am.*, **35**, 33–38.
- Olson, R.V. & Ellis, R., 1982. Iron, in *Methods of Soil Analysis, Part 2, Chemical and Microbiological Properties*, pp. 301–312, ed. Page, A.L., *Agronomy Monograph No. 9*, American Society of Agronomy–Soil Science Society of America, Madison, WI.
- Parfitt, R.L., 1989. Optimum conditions for extraction of Al, Fe, and Si from soils with acid oxalate, *Comm. Soil Sci. Plant Anal.*, **20**, 801–816.
- Phillips, E.J.P. & Lovley, D.R., 1987. Determination of Fe (III) and Fe (II) in oxalate extracts of sediments, *J. Soil Sci. Soc. Am.*, **51**, 938–941.
- Pinheiro-Dick, D. & Schwertmann, U., 1996. Microaggregates from oxisols and inceptisols: dispersion through selective dissolutions and physicochemical treatments, *Geoderma*, **74**, 49–63.
- Rozan, T.F., Benoit, G. & April, R.H., 1997. A selective dissolution analysis optimized for measurement of weathering products in a soil, *J. Soil Sci. Soc. Am.*, **61**, 949–958.
- Schofield, R.K., 1949. Effect of pH on electric charges carried by clay particles, *J. Soil Sci.*, **1**, 1–8.
- Schwertmann, U., 1959. Die fraktionierte Extraktion der freien Eisenoxide in Boden, ihre mineralogischen Formen und ihre Entstehungsweisen, *Z. Pflanzenernährung, Düngung Bodenkunde*, **84**, 194–202.
- Schwertmann, U., 1964. Differenzierung der Eisenoxide des Bodens durch photochemische Extraktion mit saurer Ammoniumoxalat-Lösung, *Z. Pflanzenernährung, Düngung Bodenkunde*, **105**, 194–202.
- Schwertmann, U., 1973. Use of oxalate for Fe extraction from soils, *Can. J. Soil Sci.*, **53**, 244–246.
- Schwertmann, U. & Cornell, R.M., 1991. *Iron Oxides in the Laboratory—Preparation and Characterisation*, VCH Publishers, Weinheim.
- Schwertmann, U., Schulze, D.G. & Murad, E., 1982. Identification of ferrihydrite in soils by dissolution kinetics, differential X-ray diffraction, and Mössbauer spectroscopy, *J. Soil Sci. Soc. Am.*, **46**, 869–875.
- Schwertmann, U., Cambier, P. & Murad, E., 1985. Properties of goethites of varying crystallinity, *Clays Clay Min.*, **33**, 369–378.
- Stumm, W. & Sulzberger, B., 1992. The cycling of iron in natural environments: considerations based on laboratory studies of heterogeneous redox processes, *Geochim. Cosmochim. Acta*, **56**, 3233–3257.
- Sulzberger, B., Suter, D., Siffert, C., Banwart, S. & Stumm, W., 1989. Dissolution of Fe (III) (hydr) oxides in natural waters; laboratory assessment on the kinetics controlled by surface coordination, *Mar. Chem.*, **28**, 127–144.
- Sun, W., Banerjee, S.K. & Hunt, C.P., 1995. The role of maghemite in the enhancement of magnetic signal in the Chinese loess-paleosol sequence: an extensive rock magnetic study combined with citrate-bicarbonate-dithionite treatment, *Earth planet. Sci. Lett.*, **133**, 493–505.
- Suter, D., Siffert, C., Sulzberger, B. & Stumm, W., 1988. Catalytic dissolution of iron (III) (hydr) oxides by oxalic acid in the presence of Fe (II), *Naturwissenschaften*, **75**, 571–573.
- Tamm, O., 1922. Eine Methode zur Bestimmung der anorganischen Komponenten des Gelkomplexes in Boden, *Medd. Statens Skogsförsöksanstalt*, **19**, 385–404.
- Tamm, O., 1932. Über die Oxalatmethode in der chemischen Bodenanalyse, *Medd. Statens Skogsförsöksanstalt*, **27**, 1–20.
- Torrent, J., Schwertmann, U. & Schulze, D.G., 1980. Iron oxide mineralogy of some soils of two river terrace sequences in Spain, *Geoderma*, **23**, 191–208.
- van Oorschot, I.H.M. & Dekkers, M.J., 1999. Dissolution behaviour of fine-grained magnetite and maghemite in the citrate-bicarbonate-dithionite extraction method, *Earth planet. Sci. Lett.*, **167**, 283–295.
- Verosub, K.L., Fine, P., Singer, M.J. & TenPas, J., 1993. Pedogenesis and paleoclimate: interpretation of the magnetic susceptibility record of Chinese loess-paleosol sequences, *Geology*, **21**, 1011–1014.
- Vlag, P., Rochette, P. & Dekkers, M.J., 1996. Some additional hysteresis parameters for a natural (titano) magnetite with known grain size, *Geophys. Res. Lett.*, **23**, 2801–2806.
- Walker, A.L., 1983. The effects of magnetite on oxalate- and dithionite-extractable iron, *J. Soil Sci. Soc. Am.*, **47**, 1022–1026.

## APPENDIX A: EXTRACTION MECHANISM OF THE AAO VERSUS THE AAO-Fe(II) EXTRACTION METHOD

### A1 AAO mechanism

The acid-ammonium oxalate extraction mechanism (Schwertmann 1964) is a ligand-promoted dissolution. As shown in Fig. A1(a), oxalate adsorbs to an Fe<sup>3+</sup> site at the crystal surface. The high polarity of the oxalate leads to a weakening of the bonds between the Fe<sup>3+</sup> and the solid, resulting in the slow release of the iron-oxalate complex into the solution. pH is an important factor in the AAO mechanism; protons facilitate the dissolution process by protonating OH groups on the mineral surface, thereby contributing to a weakening of the Fe–O bond. Thus, a decrease in pH will increase the dissolution rate. However, a decrease in pH increases the protonation of ligands in solution, thus a decrease in pH will decrease the adsorption of ligands to the mineral surface. As a result of these opposing processes, the AAO method has an optimum pH range of 2–4, where dissolution is maximum (Cornell & Schwertmann 1996).

Another influence on the pH is the presence of calcium carbonate in samples. When calcium carbonate is present in a sample, it will buffer the acid from the extraction solution and thus increase the pH. At pH values above 3, the rate of dissolution of iron will rapidly decrease (e.g. Parfitt 1989; Del Campillo & Torrent 1992). A simple calculation, assuming all acid in the extraction solution is used for the reaction of carbonate to CO<sub>2</sub>, indicates that the calcium carbonate has to be present in amounts greater than 10 wt per cent to buffer the system completely. When calcium carbonate concentrations exceeds 10 wt per cent, it is advisable to add more oxalic acid to the solution until the pH has stabilized at 3 (Del Campillo & Torrent 1992).

In the method proposed by Schwertmann (1964), the dissolution rate changes with time. As shown in Fig. A2, the dissolution rate increases considerably after an initial period of slow dissolution (Fischer 1972; Borggaard 1990; Hering & Stumm 1990). This change in dissolution rate is related to the increased concentration of Fe<sup>2+</sup> in solution, which has a catalytic effect on the dissolution mechanism (Borggaard 1981). The Fe<sup>2+</sup> combines with the oxalate in solution to form a complex that can dissolve iron from the solid more easily than an oxalate ion on its own. The oxalate in the complex acts as a bridging ligand for the electron transfer between the Fe(II) of the complex and the Fe(III) in the solid surface. After dissolution of the iron from the solid, the Fe<sup>2+</sup> will be released into the solution and can combine again with oxalate to form a new complex, which in turn can be used in the dissolution of more iron from the solid surface. By addition of a small amount of Fe<sup>2+</sup> to the extraction solution at the start of the experiment, the initial slow rate of the AAO method disappears

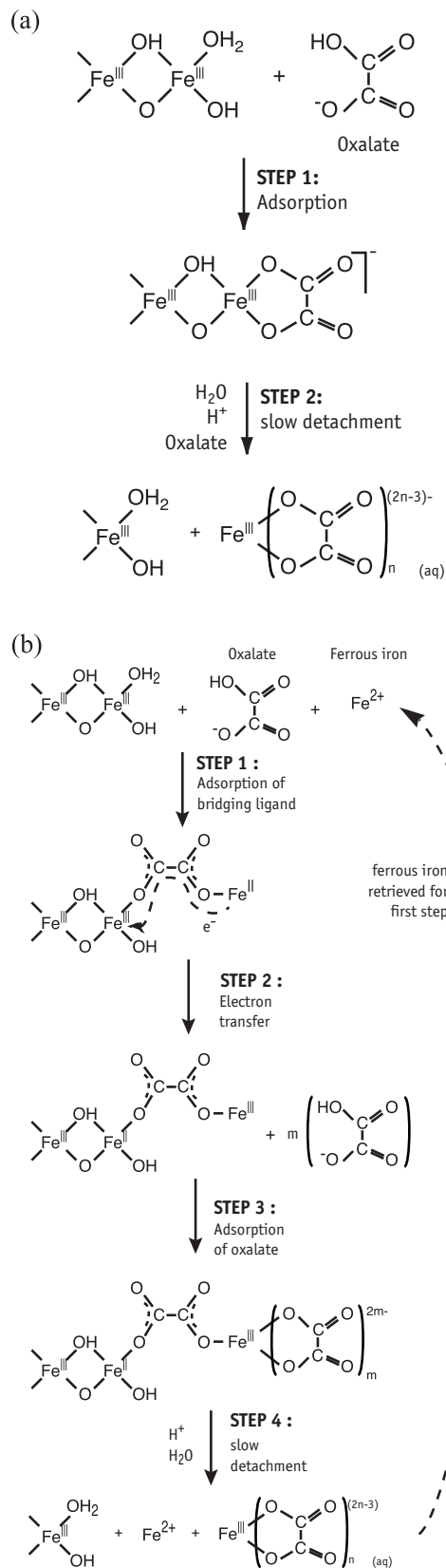


**Figure A1.** Difference in dissolution mechanism for the AAO extraction technique (a) and the AAO-Fe(II) extraction technique (b), where  $\text{Fe}^{2+}$  is added to the extraction solution at the start of the experiment (modified after Hering & Stumm 1990).

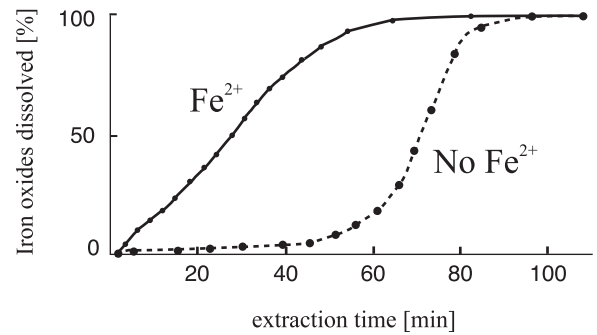


**Figure A2.** Difference in dissolution rate caused by a change of extraction mechanisms for extraction of magnetite performed with a solution containing  $0.1 \text{ mol L}^{-1}$  oxalic acid and  $6 \times 10^{-6} \text{ mol L}^{-1}$   $\text{Fe}^{2+}$  (solid line) and a similar solution without  $\text{Fe}^{2+}$  added at the start of the experiment (dotted line) (modified after Baumgartner *et al.* 1983).

(Fischer 1972; Baumgartner *et al.* 1983; Cornell & Schindler 1987; Suter *et al.* 1988; Sulzberger *et al.* 1989; Borggaard 1990; Hering & Stumm 1990; Stumm & Sulzberger 1992). Here, we refer to the adapted method, using  $\text{Fe}^{2+}$  as a catalyst, as the AAO-Fe(II) method.

## A2 AAO-Fe(II) mechanism

This dissolution mechanism has been described several times (Cornell & Schwertmann 1996) and is shown in Fig. A1(b). The addition of  $\text{Fe}^{2+}$  to the extraction solution promotes the iron oxide dissolution because the Fe(II)–oxalate complex is a strong reductant. At low pH, both the  $\text{Fe}^{2+}$  and the surface of iron oxides are positively charged and repel each other electrostatically. The charge reversal of  $\text{Fe}^{2+}$  due to its complexation with oxalate enables adsorption of the complex with the solid. The first step in the AAO-Fe(II) dissolution mechanism is the formation of a complex between  $\text{Fe}^{2+}$  and oxalate in solution. This complex adsorbs to an Fe(III) site on the mineral surface. The newly formed inner-sphere complex shifts the electron density towards the Fe(III) on the mineral surface and facilitates electron transfer with oxalate as the bridging ligand between the two iron atoms (Baumgartner *et al.* 1983; Cornell & Schindler 1987; Stumm & Sulzberger 1992). The reduced iron complex at the mineral surface can then be detached.

## APPENDIX B: GLOSSARY OF MAGNETIC TERMS USED IN THIS PAPER

- $B_c$  coercivity [mT]  
= the reverse field required to reduce the magnetization to zero from saturation
- $B_{cr}$  coercivity of remanence [mT]  
= the reverse field required to reduce the remanent magnetization to zero after saturation
- $M_{rs}$  saturation isothermal remanent magnetization [ $\text{Am}^2 \text{ kg}^{-1}$ ]  
= the magnetization remaining in the absence of an external magnetic field after saturation
- $M_s$  saturation magnetization [ $\text{Am}^2 \text{ kg}^{-1}$ ]  
= the strongest possible magnetization which can be produced in a specimen by applying a field
- $\chi$  specific susceptibility [ $\text{m}^3 \text{ kg}^{-1}$ ]  
= low-field magnetic susceptibility expressed in terms of unit mass